Some design issues for 3C-3D OBC seismic data

Don C. Lawton and Brian H. Hoffe

ABSTRACT

Depth-specific conversion point (DSCP) mapping is superior to asymptotic conversion point (ACP) mapping for 3C-3D seismic survey design. P-S fold patterns at target levels depend on V_p/V_s, and in the case of ocean bottom cable (OBC) data, also on water depth. These issues are illustrated in a simple design example.

INTRODUCTION

Over the past several years, CREWES has discussed a number of design issues for both 2D and 3D converted-wave surveys (Lawton, 1993, 1994, 1996; Lawton et al., 1995). Initially, survey designs were based only on asymptotic conversion points, and the major issues revolved around bin size and fold periodicity resulting from asymptotic binning approaches (Lawton, 1993, 1994). More recently, studies incorporated depth-specific binning algorithms that mapped the true depth-variant position of conversion points for the same source-receiver offset (Lawton et al., 1995, Lawton, 1996). These studies were also directed at land 3C-3D surveys, for which the total source effort is typically about a factor of 2 or 3 times the total receiver effort.

With recent advances in ocean-bottom-cable (OBC) 4-component (4C) acquisition technology, there has been an explosive growth of converted wave surveys in the marine environment. The purpose of these surveys has been for structural imaging in areas with gas chimneys such as the Tommeliten field, North Sea (Granli et al., 1999), and more recently, for stratigraphic and lithological mapping at the Alba field, also in the North Sea (MacLeod et al., 1999). Because of the high cost of deployment of OBC systems and the low cost per shot in the marine environment, these converted-wave surveys have a very high source to receiver effort ratio. In addition, since the receivers are placed on the ocean floor, the receivers and shots are vertically separated, with this elevation difference becoming significant for deep water surveys currently being reported. These factors require consideration at the design stage, and CREWES software is being developed to evaluate their importance.

OBC 3C-3D DESIGN EXAMPLE

Some design issues for 3C-3D OBC data are best illustrated through an example. A synthetic survey design was developed using parameters listed in Table 1, representing a typical small survey. The receiver patch covers an area of 2.0 × 1.5 km, located centrally in a shot patch which measures 4.0 × 3.0 km in area. Figure 1 shows the design geometry; shots extend well outside the areal extent of the receiver patch to get good offset and azimuth distributions for converted waves within the area covered by receivers. This survey was designed for a target depth of 2000 m.

P-P fold maps

Figure 2 shows the conventional P-P fold map for this survey, for all azimuths, and for source-receiver offsets from 0 to 2500 m. In this example, the shot and receivers are modelled to be at the same elevation. As expected, the fold is greatest at the centre of the survey, reaching a maximum value of 120, and tapers smoothly towards the outside of the receiver patch.

Table 1. Source and receiver parameters for example 3C-3D OBC design.

Source Data	Parameter
Number of Source Lines	41
Source Line Separation	100 m
Number of source points/line	61
Source Interval	50 m
Source Line Orientation	0º
Total Number of Source Points	2501
Receiver Data	**Parameter**
Number of Receiver Lines	6
Receiver Line Separation	300 m
Number of receiver points/line	41
Receiver Interval	50 m
Receiver Line Orientation	90º
Total Number of Receiver Points	246
Bin Dimensions	25 × 25 m
Source/Receiver Effort	10.17

In comparison, Figure 3 shows a P-P fold map using the identical parameters as shown in Figure 2, except that the receivers are placed 200 m below the source plane (representing an OBC survey in a water depth of 200 m). The fold map shows stripes with higher fold parallel to the receiver lines, and stripes with lower fold parallel to the shot lines. One might expect an acquisition footprint to be evident in P-wave data recorded using this geometry. Although this fold map was computed assuming a single, homogeneous layer with no ray-bending of the downgoing P-wave across the seafloor, it does illustrate that water depth (in this case 10% of the target depth) will impact P-wave illumination patterns at the target.

P-S fold maps

Figure 4 is the P-S fold map, computed using asymptotic binning, for $V_p/V_s = 2.0$, and placing the source and receivers at the same elevation. This map shows stripes of

empty bins parallel to the shot lines (for bin dimensions of 25 × 25 m), as predicted from criteria discussed by Lawton (1994). However, a more accurate view of the subsurface P-S illumination is provided by generating a depth-specific fold map, shown in Figure 5. These data are computed by ray-tracing through a single homogeneous layer with $V_p/V_s = 2.0$ and retaining the source and receiver to be at the same elevation, and for a target depth of 2000 m. The depth-specific fold map (Figure 5) predicts a smoother fold variation than the asymptotic fold map (Figure 4), although there is still some lower fold bin lines parallel to the shot lines. The near and far offset displays of this acquisition design are shown in Figures 6 and 7, respectively; these show acceptable near and far offset distributions.

In the case of OBC data, the receivers are placed at the sea floor, and the change in elevation between sources and receiver will alter the P-S binning characteristics. Figures 8 through 10 show the depth-specific (target depth of 2000 m) fold maps for water depths of 100 m, 200 m and 400 m respectively. As the water depth increases, the long-wavelength fold-variations become more pronounced, parallel to the receiver lines and generally between them. Although the maximum fold is high (around 180), the pattern of fold variations might be anticipated to result in a discernible acquisition footprint in processed data volumes. This poor fold pattern could be ameliorated by using a smaller receiver line separation (e.g. 150 m).

The fold maps in Figures 8 through 10 were all computed for $V_p/V_s = 2.0$. The fold distribution will also depend on the value of V_p/V_s. Figures 11 and 12 show the fold distribution for V_p/V_s of 1.5 and 2.5 respectively. These are minimum and maximum values that would be expected in most sedimentary basins. An important observation is that the total area illuminated by P-S waves decreases as V_p/V_s increases (the conversion point moving closer to the receiver as V_p/V_s increases). As seen in Figure 12, the fold pattern becomes smoother as V_p/V_s increases and shows maximum high-frequency variation for lower V_p/V_s values (Figure 11).

Discussion and continuing development

The P-S fold maps presented illustrate that V_p/V_s and water depth as a function of target depth will both introduce patterns of fold variations that might yield acquisition footprints in P-S volumes from OBC surveys. It is planned to continue this modelling work to incorporate layered models and well as anisotropic velocities.

REFERENCES

Granli, J. R., Arnsten, B., Anders, S. and Hilde, E. 1999, Imaging through gas-filled sediments using marine shear-wave data: Geophysics, **64**, 668-677.

Lawton, D.C., 1993, Optimum bin size for converted-wave 3-D asymptotic mapping: CREWES Research Report Volume 5, 28.1-28.14.

Lawton, D.C., 1994, Acquisition design for 3-D converted waves: CREWES Research Report Volume 6, 23.1-23.23.

Lawton, D.C., Stewart, R.R., Cordsen, A., and Hrycak, S., 1995, Advances in 3C-3D design for converted waves: CREWES Research Report Volume 7, 43.1-43.41.

Lawton, D.C, 1996, Design review of the Blackfoot 3C-3D seismic survey: CREWES Research Report Volume 8, 38.1-38.23.

MacLeod, M. K., Hanson, R. A., Hadley, M. J., Reynolds, K. J., Lumley, D., McHugo, S., and Probert, A., 1999, The Alba field OBC seismic survey: 61st EAGE Mtg, Exp. Abstracts, No. 6-25.

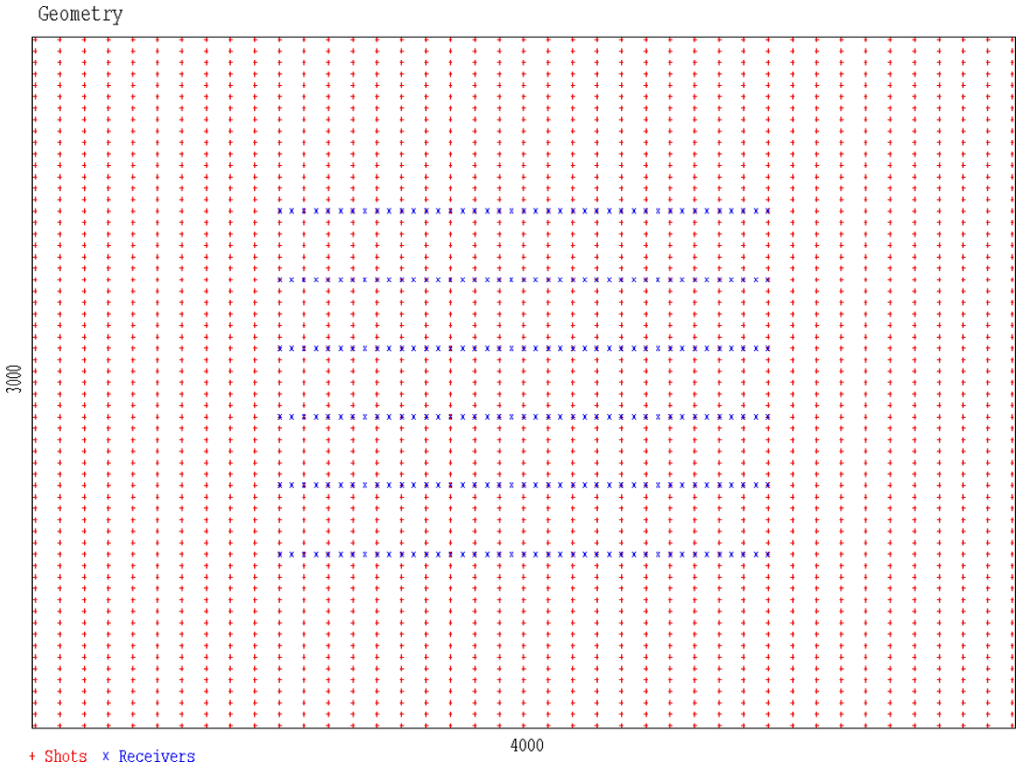

Figure 1. Source and receiver geometry for example 3C-3D OBC design

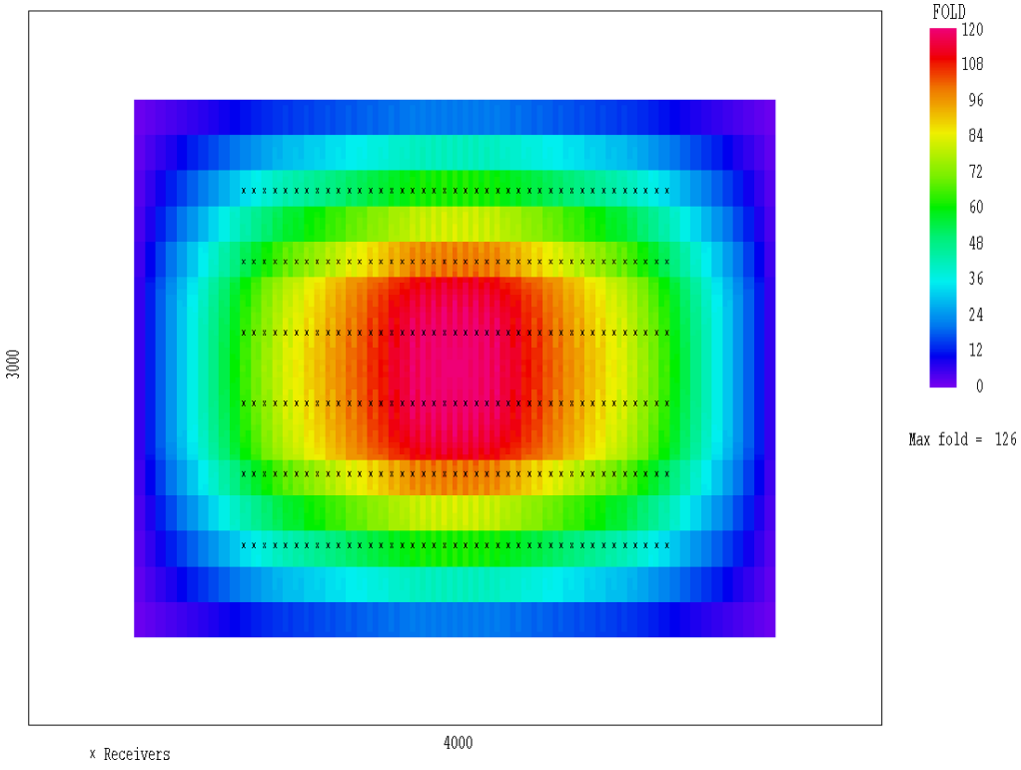

Figure 2. Conventional P-P fold for example OBC design for all azimuths and source-receiver offsets limited to 2500 m.

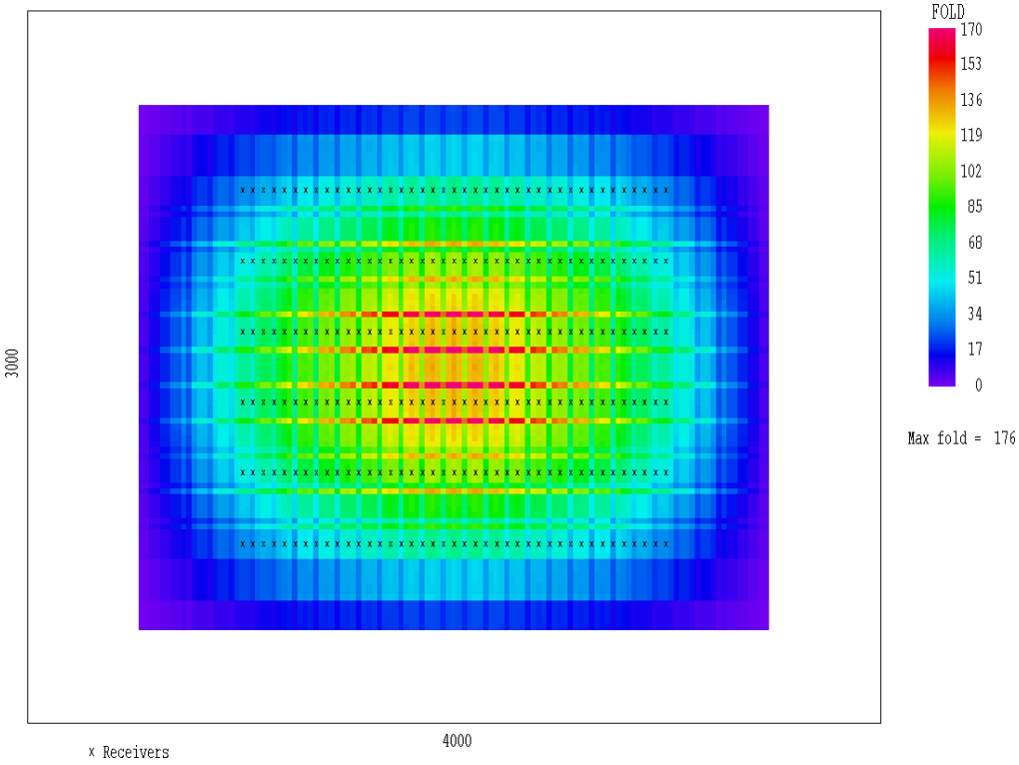

Figure 3. P-P fold using identical parameters as shown in Figure 2, except receivers are now placed 200 m below the source plane to represent an OBC survey in 200 m water depth.

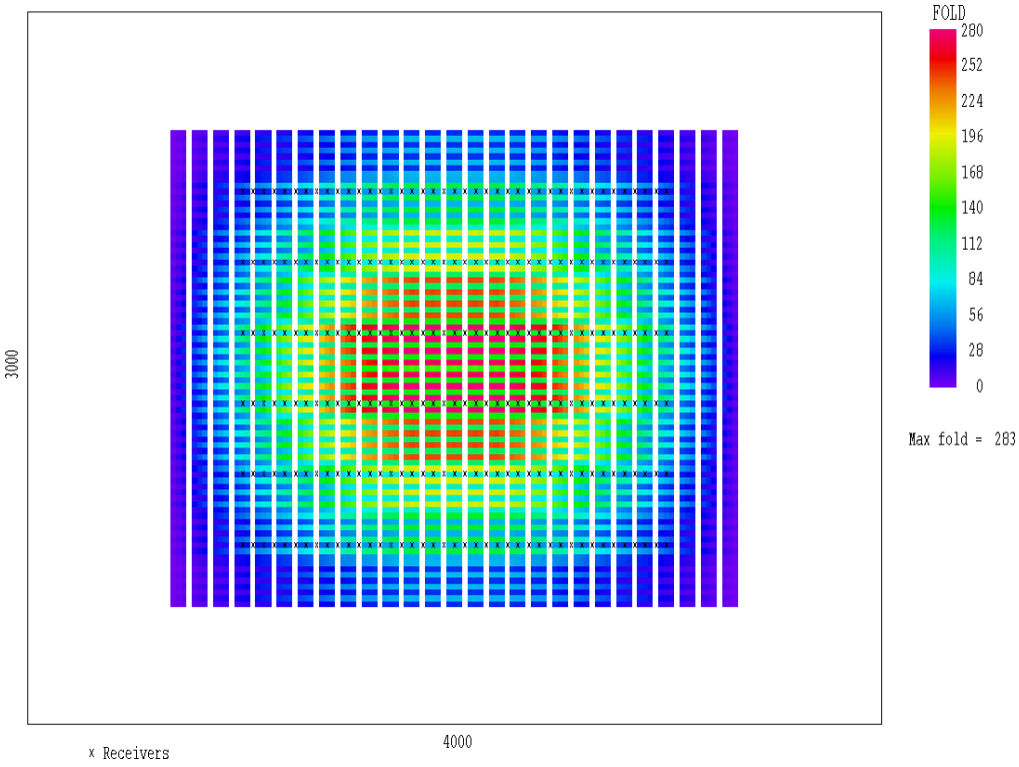

Figure 4. Asymptotic conversion point (ACP) P-S fold computed for V_p/V_s = 2.0 with source and receivers at the same elevation.

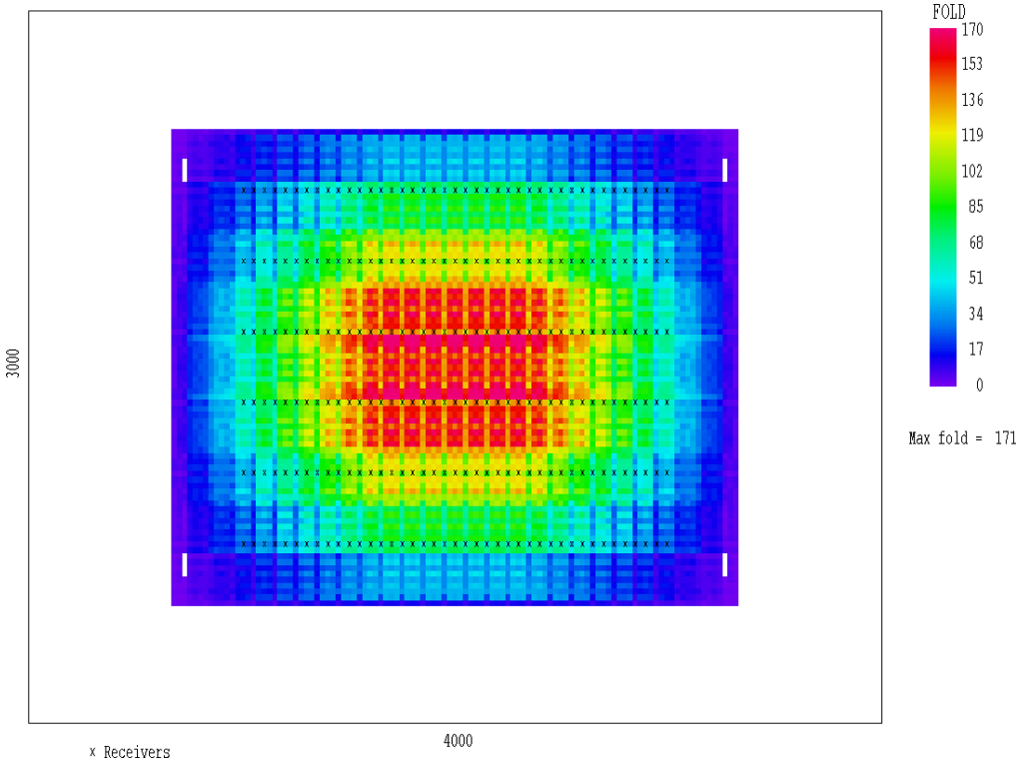

Figure 5. Depth-specific conversion point (DSCP) P-S fold for a target depth of 2000 m. These data are computed by raytracing through a single homogeneous layer with $V_p/V_s = 2.0$ and retaining the source and receiver at the same elevation.

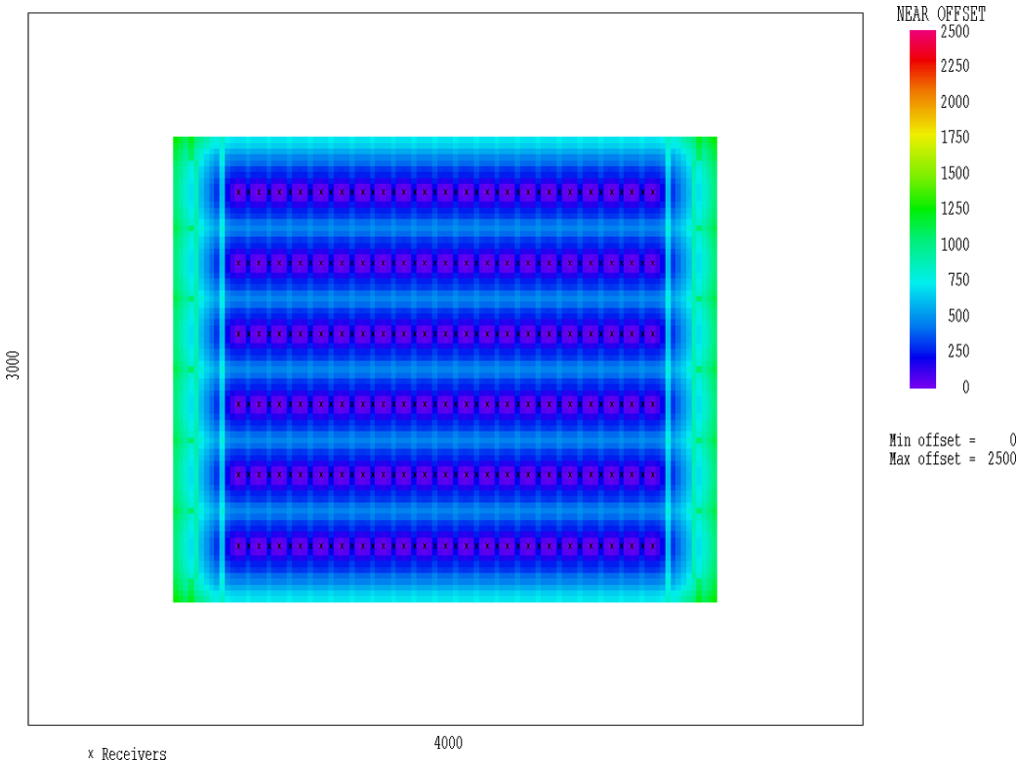

Figure 6. Near offset distribution for the acquisition design presented in Figure 5.

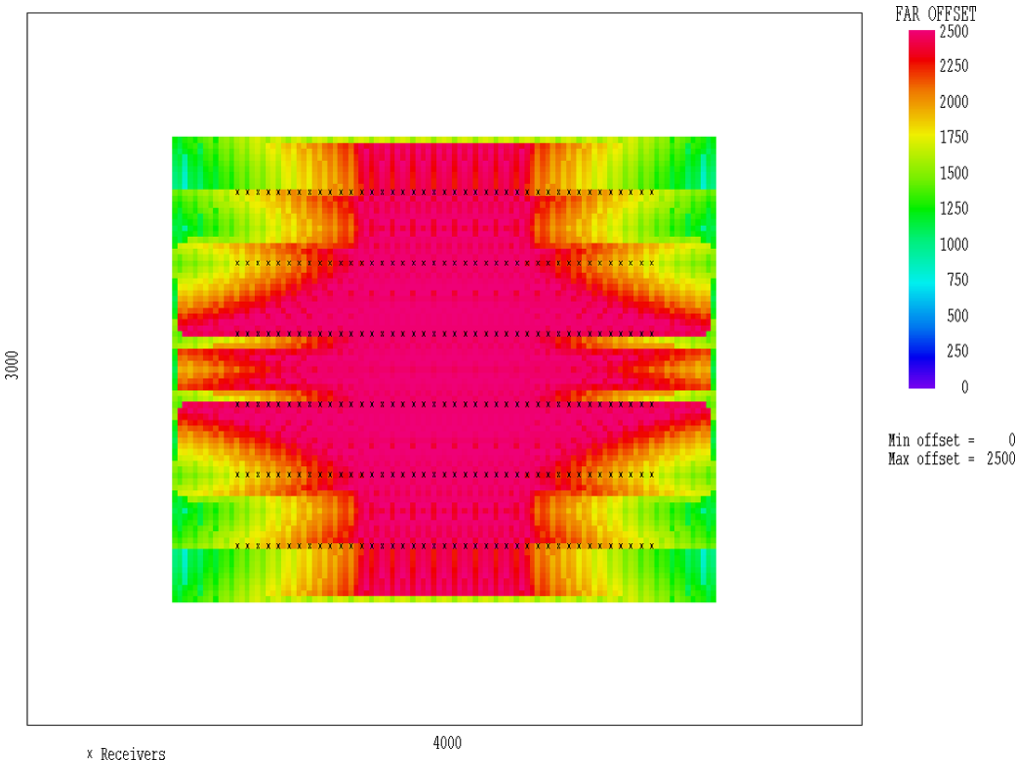

Figure 7. Far offset distribution for the acquisition design presented in Figure 5.

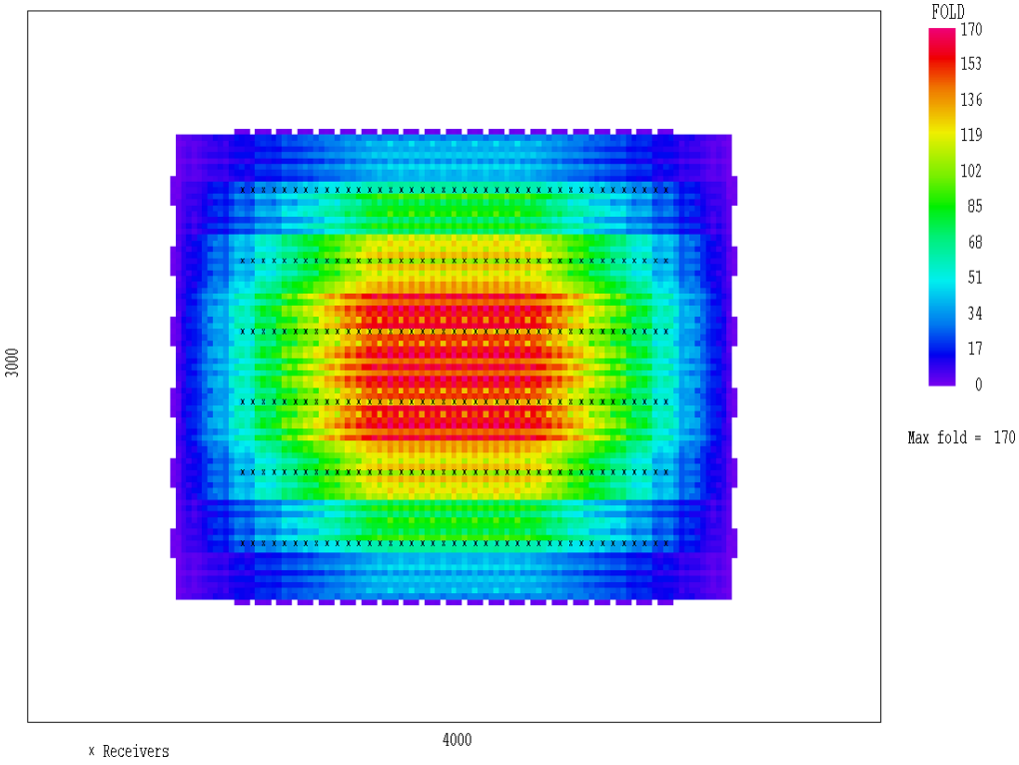

Figure 8. Depth-specific conversion point (DSCP) P-S fold for V_p/V_s = 2.0 , target depth = 2000 m and water depth = 100 m.

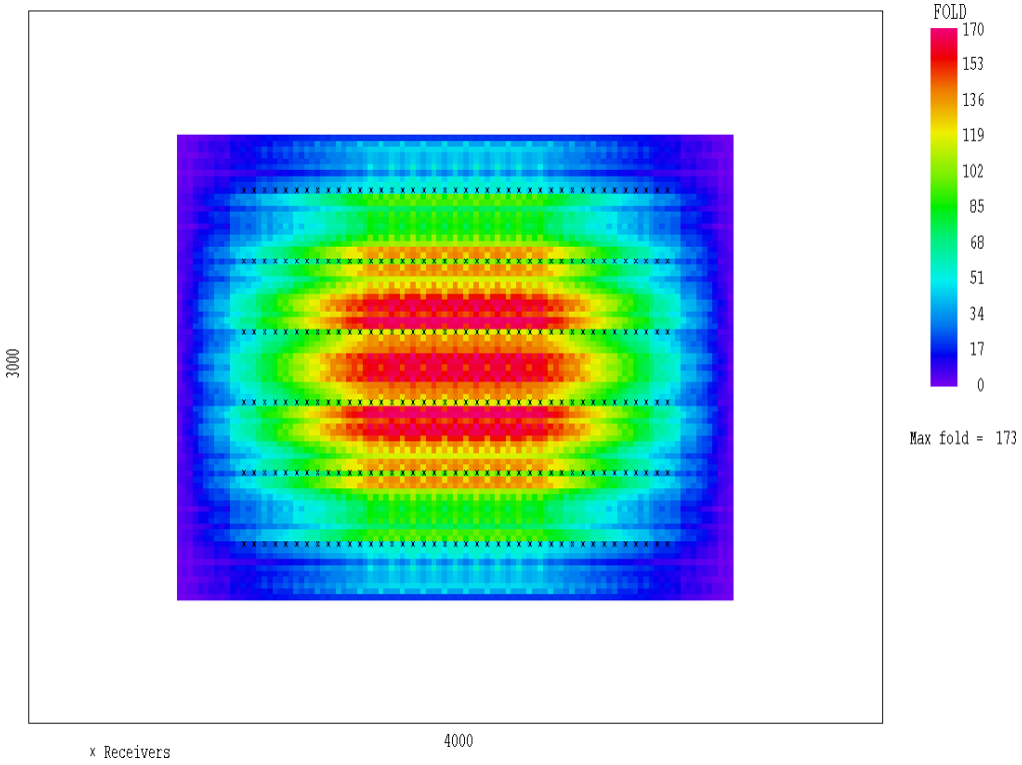

Figure 9. Depth-specific conversion point (DSCP) P-S fold for V_p/V_s = 2.0 , target depth = 2000 m and water depth = 200 m.

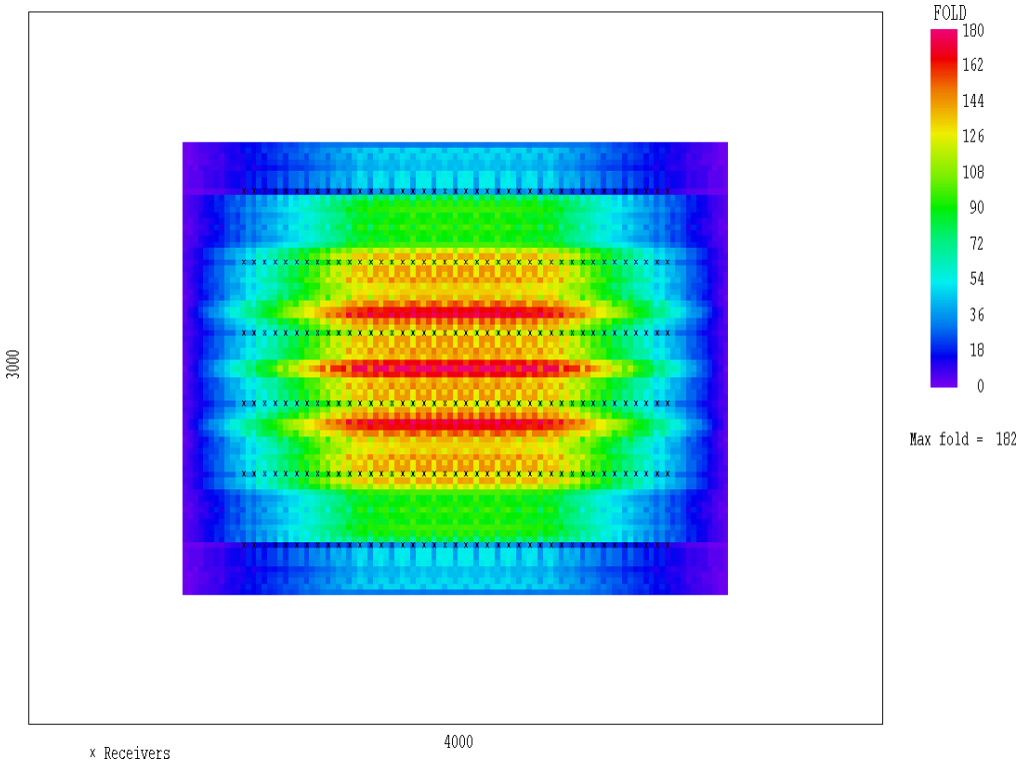

Figure 10. Depth-specific conversion point (DSCP) P-S fold for V_p/V_s = 2.0 , target depth = 2000 m and water depth = 400 m.

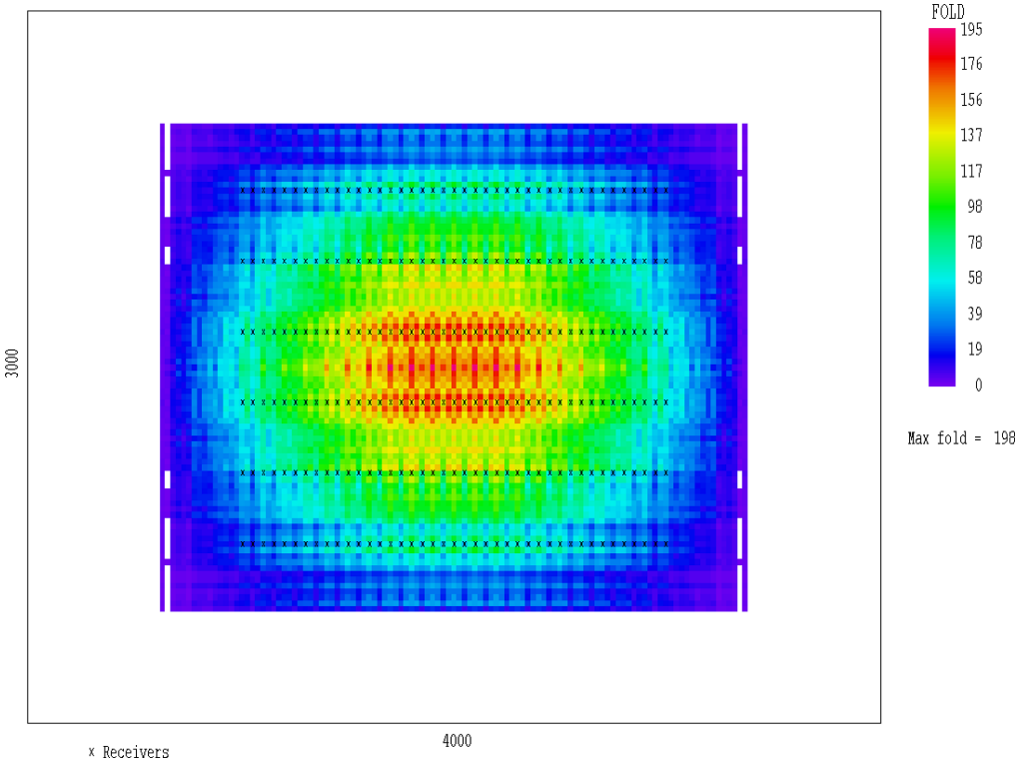

Figure 11. Depth-specific conversion point (DSCP) P-S fold for V_p/V_s = 1.5 , target depth = 2000 m and water depth = 200 m.

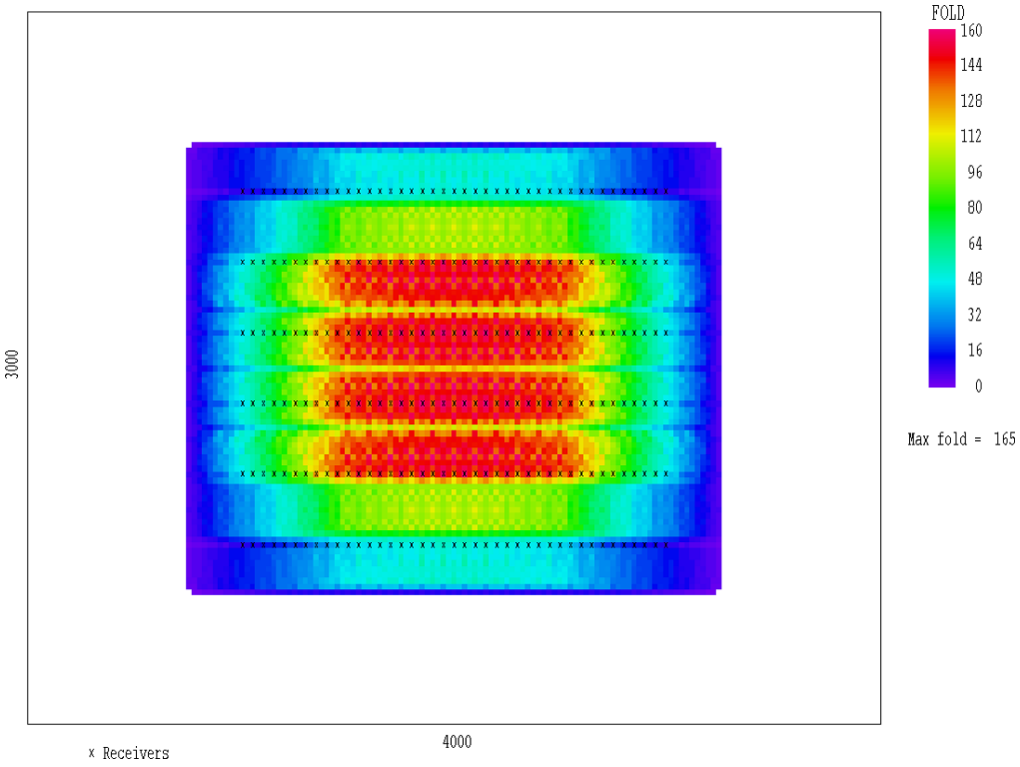

Figure 12. Depth-specific conversion point (DSCP) P-S fold for V_p/V_s = 2.5 , target depth = 2000 m and water depth = 200 m.